BIOMICROFLUIDICS **12**, 044110 (2018)

Microfluidic on-chip immunohistochemistry directly from a paraffin-embedded section

Chang Hyun Cho,[1] Seyong Kwon,[1] Segi Kim,[1] Yoonmi Hong,[1] Pilnam Kim,[1] Eun Sook Lee,[2] and Je-Kyun Park[1,a)]
[1]*Department of Bio and Brain Engineering, Korea Advanced Institute of Science and Technology (KAIST), 291 Daehak-ro, Yuseong-gu, Daejeon 34141, Republic of Korea*
[2]*Center for Breast Cancer, National Cancer Center, 323 Ilsan-ro, Ilsandong-gu, Goyang-si, Gyeonggi-do 10408, Republic of Korea*

(Received 31 May 2018; accepted 9 July 2018; published online 19 July 2018)

We present here a novel microfluidic platform that can perform microfluidic on-chip immunohistochemistry (IHC) processes on a formalin-fixed paraffin-embedded section slide. Unlike previous microfluidic IHC studies, our microfluidic chip made of organic solvent-resistant polyurethane acrylate (PUA) is capable of conducting on-chip IHC processes consecutively. A narrow channel wall structure of the PUA chip shows effective sealing by pressure-based reversible assembly with a section slide. We performed both on-chip IHC and conventional IHC processes and compared the IHC results based on the immunostaining intensity. The result showed that the effects of the on-chip deparaffinization, antigen retrieval, and immunoreaction processes on the IHC result were equivalent to conventional methods while reducing the total process time to less than 1/2. The experiment with breast cancer tissue shows that human epidermal growth factor receptor 2 (HER2) classification can be performed by obtaining a clearly distinguishable immunostaining intensity according to the HER2 expression level. We expect our on-chip microfluidic platform to provide a facile technique suitable for miniaturized, automated, and precise diagnostic devices, including a point-of-care device. *Published by AIP Publishing.*
https://doi.org/10.1063/1.5042347

INTRODUCTION

Immunohistochemistry (IHC) is a well-known and widely used technique in histopathology for the detection of target biomarkers by specific binding of the antibody to the target antigen on tissues or cells. This technique provides various kinds of cellular and molecular information, such as localization,[1] morphological characteristics,[2] subtype,[3] and level of biomarker expression.[3,4] Immunohistochemically processed tissues or cells can be qualitatively and quantitatively analyzed by pathologists and classified based on the type and status of the disease to determine a clinical treatment method.[5–8] For this reason, IHC is being considered as a gold standard in clinical diagnosis and prognosis. As our understanding of complex molecular interactions of cancer has increased, the need for an improved diagnosis tailored to each individual case has increased.[9,10] The analysis of multiple biomarkers related to tumorigenesis is also required to accurately characterize the type of cancer, leading to an increased demand for a large number of different assays. An automated IHC machine, which can automatically perform whole IHC processes with a simple operation, has been introduced to rapidly handle a large number of sample slides;[11,12] however, it is inefficient for analyzing small amounts of samples such as rare or small-scale tissue biopsies by one IHC condition on a slide. It also has the difficulty in integrating with another molecular analysis platform for in-depth biological studies.

[a)]Author to whom correspondence should be addressed: jekyun@kaist.ac.kr. Tel.: +82-42-350-4315. Fax: +82-42-350-4310.

In this respect, the integration of the microfluidic platform for biochemical analysis has been provided to solve these issues. The small dimension of the microfluidic environment provides a high surface-to-volume ratio that enhances the antibody–antigen reaction of the immunoassay, the precise control of the fluid, the reduced sample and reagent consumption, and the ease of development of the multiplexed network of the microchannel.[13,14] These advantages have led to the development of various microfluidic IHC platforms that are capable of performing complex assays, such as multiplexed biomarker screening on breast cancer tissue,[15,16] precise spatial control of immunostaining,[17,18] and enhanced immunoreaction in a reduced process time.[19] An accurate IHC analysis for biomarker quantification was also demonstrated using a quantum-dot based microfluidic double-staining method,[20,21] a microfluidic tissue processor for formalin-fixed sections,[22] and frozen sections,[23] and standardization of immunostaining quality.[24]

Although these microfluidic techniques have contributed to expand the potential of the IHC process, there are still a limited number of applications. This is due to the fact that most microfluidic IHC techniques are only applied to the immunostaining process of the entire IHC process, excluding the deparaffinization and antigen retrieval processes. Because elastic polymers such as poly(dimethylsiloxane) (PDMS) used in the fabrication of microfluidic devices are generally vulnerable to organic solvents, they can cause swelling or failure of the device during the deparaffinization process.[25] A recent study has shown that deparaffinization and immunostaining processes are performed using a microfluidic probe in an open space platform;[26] however, the replacement of immersion fluid is required to perform each process, thereby complicating the manipulation. In addition, the method specialized for micro-scale staining is not suitable for whole slide staining.

In this research, we demonstrated for the first time a novel microfluidic platform that can perform on-chip IHC processes in a microfluidic environment. To provide on-chip IHC processes in an organic solvent-resistant device, our microfluidic chip is fabricated using polyurethane acrylate (PUA), which has chemical resistance against organic solvents.[27] A narrow channel wall structure of the PUA chip reduces the contact area between the chip and the sample slide, thereby reducing the pressure required to seal the chip by pressure-based reversible assembly. After assembling with a formalin-fixed paraffin-embedded (FFPE) sample section and a chip, deparaffinization, antigen retrieval, and immunoreaction processes are carried out continuously (Fig. 1). Based on on-chip IHC processes, we characterized the effectiveness of each on-chip process and compared to conventional IHC results by manual pipetting using cancer cell block-section slides. The diagnostic capability of our platform has also been verified using breast cancer tissue.

MATERIALS AND METHODS

Design and fabrication of an organic solvent-resistant microfluidic chip

A microfluidic PUA chip consists of a reaction chamber where reagents react with the sample section and two distributing channels that distribute and withdraw injected reagents [Fig. 2(a)].

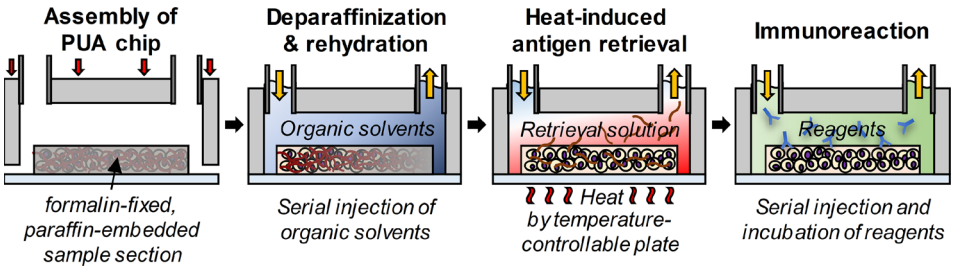

FIG. 1. Schematics of the overall processes of on-chip immunohistochemistry within an assembly. A microfluidic chip made of PUA is assembled with an FFPE section slide by a pressure-based reversible sealing method. On-chip deparaffinization is performed by serial injection of organic solvents, including xylene and ethanol solutions with different concentrations. A temperature-controllable plate beneath the section slide generates heat to perform heat-induced antigen retrieval while injecting the retrieval solution into the chip. Immunoreaction is performed by serial injection and incubation of the reagents using a syringe pump.

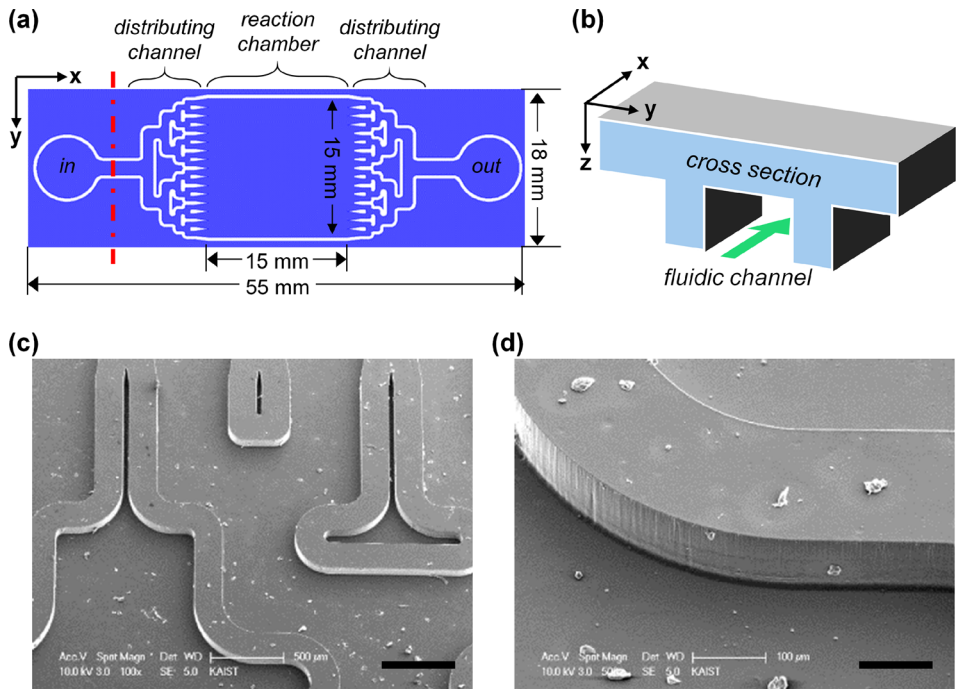

FIG. 2. Configuration of a wall-structured microfluidic PUA chip. (a) Dimension and configuration of a wall-structured microfluidic chip. (b) The schematic cross section along the red line of (a) shows a narrow wall structure that reduces the contact area with the section slide. SEM images show (c) a top view and (d) a tilted view of the wall-structured PUA chip. As shown, the narrow channel wall structure of the PUA chip was successfully fabricated by two consecutive replica molding processes [scale bars: 500 μm for (c) and 100 μm for (d)].

The dimension of the reaction chamber is 15 mm × 15 mm × 300 μm ($w \times l \times h$), which can cover a whole tissue/cell section. An ultraviolet (UV)-curable PUA resin, MINS 301RM, was purchased from Minuta Technology (Osan, Korea). The PDMS precursor Sylgard 184 and the curing agent were purchased from Dow Corning (Midland, MA, USA). The polycarbonate mold for the PDMS replica molding was fabricated by micromilling. Due to the rigid characteristics of the cured PUA, it is difficult to obtain a cured PUA chip by direct replica molding from a rigid master mold such as polycarbonate. Therefore, to overcome this limitation, two consecutive replica molding processes were performed: (1) polycarbonate mold to PDMS and (2) PDMS mold to PUA (Fig. S1 in the supplementary material). First, a mixture of a PDMS precursor and a curing agent (10:1 ratio) was poured onto a polycarbonate mold and cured for 1 h at 90 °C. The cured PDMS was used as a mold for the second replica molding process because of its elastic property, which facilitates peeling off from the cured PUA. The PUA resin was then poured onto the PDMS mold and covered with a transparent acrylic block for chip support, followed by UV radiation at 18 mJ/cm^2 for 3 h. After curing, the PDMS mold was peeled off from the cured PUA chip attached to the supporting acrylic block.

Preparation of a breast cancer cell block section

Breast cancer cell line MCF-7 and SKBR3 cells were purchased from the Korean Cell Line Bank (Seoul, Korea). Roswell Park Memorial Institute medium 1640 (RPMI 1640), fetal bovine serum (FBS), penicillin and streptomycin (PS), and phosphate buffered saline (PBS) were purchased from Corning (Corning, NY, USA). MCF-7 and SKBR3 cells were cultured in RPMI 1640 media with 10% FBS and 1% PS. All cells were incubated at 37 °C, 5% CO_2 in a humidified environment. Sufficiently cultured cells were trypsinized, harvested, and fixed with 4% formaldehyde solution diluted in PBS for 15 min at room temperature. The fixed cells were centrifuged to make a block, dehydrated with ethanol and xylene, and finally embedded with paraffin. The paraffin-embedded cell block was sectioned with a thickness of 4 μm using a microtome,

attached to the glass slide, and dried overnight at 40 °C. The MCF-7 cell block section was used for the IHC assays of cytokeratin, estrogen receptors (ERs), and progesterone receptors (PRs). The SKBR3 cell block section was used for the IHC assay of human epidermal growth factor receptor 2 (HER2).

Conventional IHC process for the control experiment

The anti-cytokeratin antibody, anti-HER2 antibody, anti-ER antibody, anti-PR antibody, and target retrieval solution were purchased from Dako (Troy, MI, USA). The antibody diluent was purchased from Life Technologies (Carlsbad, CA, USA). The horseradish peroxidase (HRP)-3,3'-diaminobenzidine (DAB) staining kit was purchased from Abcam (Cambridge, UK). Tris-buffered saline with Tween (TBS-T; 0.1% Tween 20) was purchased from ScyTek (Logan, UT, USA). An FFPE cell block section was deparaffinized and rehydrated by batch-type dipping in solvents as follows: twice in xylene for 5 min, twice in 100% ethanol for 3 min, three times in 95% ethanol diluted in distilled water for 1 min, and gently washed with distilled water. The rehydrated section was immersed in a target retrieval solution and was heated using a microwave oven in the defrost mode for 20 min to perform heat-induced antigen retrieval, which enhances the antigenicity of cells in the section. After cooling the section for 10 min at room temperature, conventional immunostaining was performed using a HRP-DAB staining kit based on the protocol: HRP block for 10 min, protein block for 10 min, primary antibody incubation for 1 h, conjugated secondary antibody incubation for 10 min, HRP conjugate incubation for 15 min, and DAB staining for 5 min. For the incubation of the primary antibody, anti-cytokeratin, anti-HER2, anti-ER, and anti-PR antibodies were diluted to 1:1000, 1:200, 1:100, and 1:100, respectively, using an antibody diluent before use. TBS-T buffer was used for every washing step.

On-chip deparaffinization and antigen retrieval processes

On-chip deparaffinization was performed as follows: an FFPE cell block section was placed on a temperature-controllable plate (Nep Engineering, Suwon, Korea) and covered with the PUA chip. A pair of lever clamps was used to tightly seal the PUA chip, the section slide, and the temperature-controllable plate. After assembly, xylene, 100% ethanol, and 95% ethanol diluted in distilled water were serially injected by a syringe pump (Harvard Apparatus, MA, USA) at a flow rate of 1 ml/min for 30 s. To minimize the solvent exchange process, the withdrawal mode of the syringe pump was used so that only the solvent to be infused was changed for continuous, serial injection of various solvents during the on-chip process. In the case of an on-chip antigen retrieval process, a deparaffinized section was assembled with the PUA chip and the temperature-controllable plate. After assembly, the temperature controllable plate heated the section slide, while injecting the target retrieval solution at a flow rate of 100 μl/min for 20 min. After heating, the section slide was cooled to room temperature while keeping the flow of the target retrieval solution for 5 min for cooling the section slide. The temperature condition was also characterized by comparing the immunostaining result while increasing the temperature starting at 65 °C.

Continuous on-chip IHC processes

A section slide was assembled with the PUA chip and the temperature-controllable plate, and on-chip deparaffinization and antigen retrieval processes were conducted on it. When injecting a new reagent and during every washing step between the incubation of each reagent, a high flow rate of 1 ml/min was used to rapidly exchange the reagent inside the chamber of the PUA chip. The flow rates of each reagent were controlled to optimize the incubation conditions. For immunostaining, 300 μl of HRP block was injected for 18 s to replace the reagent inside the reaction chamber, followed by a flow of the same reagent at 100 μl/min for 3 min. The same process was conducted for the protein block. Next, 300 μl of the diluted antibody solution was injected for 18 s, followed by a flow of the same reagent at 15 μl/min for 20 min. The conjugated secondary antibody was conducted in the same way with the HRP block and

the protein block. Then, 300 μl of HRP conjugate solution was injected for 18 s, followed by a flow of the same reagent at 60 μl/min for 5 min. Finally, the section slide was disassembled from the PUA chip and the temperature-controllable plate and treated with 200 μl of DAB solution for 5 min. For washing between each reagent of immunostaining, 300 μl of TBS-T was injected for 18 s.

Validation of the clinical application of on-chip IHC processes

Human tissue sample sections of HER2 positive breast cancer were gratefully received from the National Cancer Center (Goyang, Korea), with the corresponding written consent provided by the patients or their relatives. The thickness of human tissue sections was 5 μm. Human tissue sections were processed by our platform with the anti-HER2 antibody, and the immunostaining results were categorized based on the HER2 expression level provided by the National Cancer Center. The experimental conditions were the same with the on-chip IHC processes described above.

Image acquisition and analysis

Bright-field images of immunostained section slides were obtained on a microscope (IX51; Olympus, Tokyo, Japan) using a charge-coupled device (CCD) (DP-72; Olympus). The obtained images were analyzed using the ImageJ program (National Institutes of Health, Bethesda, MD, USA). First, the image was deconvoluted to split and remove the noise signal and to obtain only the DAB signal image. This image was filtered by a threshold value to remove backgrounds and/or a false staining signal and to obtain the immunostained cell areas of interest. Then, the immunostaining intensity was measured by averaging the intensity value of pixels of the filtered image. For on-chip deparaffinization and on-chip antigen retrieval, we normalized the immunostaining intensity of the conventional IHC result as 100 and calculated the immunostaining intensity of the on-chip IHC result. A two-sample *t*-test was performed to statistically analyze the effectiveness of the on-chip IHC method compared to the conventional IHC method.

RESULTS AND DISCUSSION

Effective sealing of the wall-structured PUA chip

One of the challenging issues with chemical resistant materials on a microfluidic chip is their rigid characteristics (elastic modulus: 19.8 MPa), which have the difficulty in bonding or sealing. For the IHC assay, we used a pressure-based reversible sealing method to seal the microfluidic channel by applying pressure on the chip that is in contact with the section slide.[19,24] However, the UV-curable PUA used in this work also has a rigid property after curing and causes a sealing problem. Since a typical microfluidic chip has a flat surface, it has a large contact area with the sample, thereby lowering the pressure applied to the channel surface. This insufficient sealing pressure resulted in a leakage of the injected reagents [Figs. S2(a) and S2(c) in the supplementary material]. Increasing the applied pressure is inapplicable because it may damage the sample underneath. To increase the sealing pressure without increasing the applying pressure, the contact area must be decreased. As shown in Fig. 2, we designed a wall-structured chip that had a narrow channel wall that significantly reduced the contact area. Using this wall-structured chip, the pressure-based reversible sealing of the PUC chip was successfully conducted without leakage [Figs. S2(b) and S2(d) in the supplementary material]. Furthermore, the reversible sealing of the wall-structured chip was also maintained after injection of xylene and ethanol. Based on these results, we expected that our wall-structured chip would provide a simple solution for pressure-based sealing problems.

Verification of on-chip deparaffinization

The effectiveness of the on-chip deparaffinization process was evaluated indirectly by comparing the immunostaining results of two groups; one is processed by on-chip deparaffinization and the other processed by conventional deparaffinization. All other IHC processes, including antigen retrieval and immunostaining, were performed identically for both groups in a

conventional manner. Four biomarkers (cytokeratin, ER, PR, and HER2) on two types of breast cancer cell sections (e.g., MCF-7, SKBR3) were used for verification. Figure 3(a) shows the images of immunostained sections processed by on-chip and conventional deparaffinization. As shown in Fig. 3(b), on-chip deparaffinization showed equal effectiveness compared to the conventional process for four biomarkers on breast cancer cell sections based on immunostaining results while reducing the process time to 1/10 (from 19 min to 2 min). The normalized immunostaining intensities of cytokeratin, ER, PR, and HER2 were 101.48 ± 0.76, 102.24 ± 1.27, 107.97 ± 15.76, and 99.75 ± 9.42, respectively. A statistical analysis was carried out using a two-sample *t*-test: $p > 0.4$ for four biomarkers. The reduced process time of on-chip deparaffinization is due to the flow of solvents in the microfluidic chip. The flows of xylene and ethanol transport the dissolved paraffin from the section slide above the diffusion limit, while the conventional deparaffinization process is limited by diffusion of paraffin. Fresh solvents that are continuously injected into the chip also keep the dissolution rate of paraffin high during the process.

Verification of on-chip antigen retrieval

Prior to comparing the effectiveness of on-chip antigen retrieval with the conventional process, the temperature condition for performing on-chip antigen retrieval was characterized. Although the range of the temperature condition is lower than that of the recommended condition (over 100 °C by a microwave oven or a pressure cooker) based on the previous studies,[28,29]

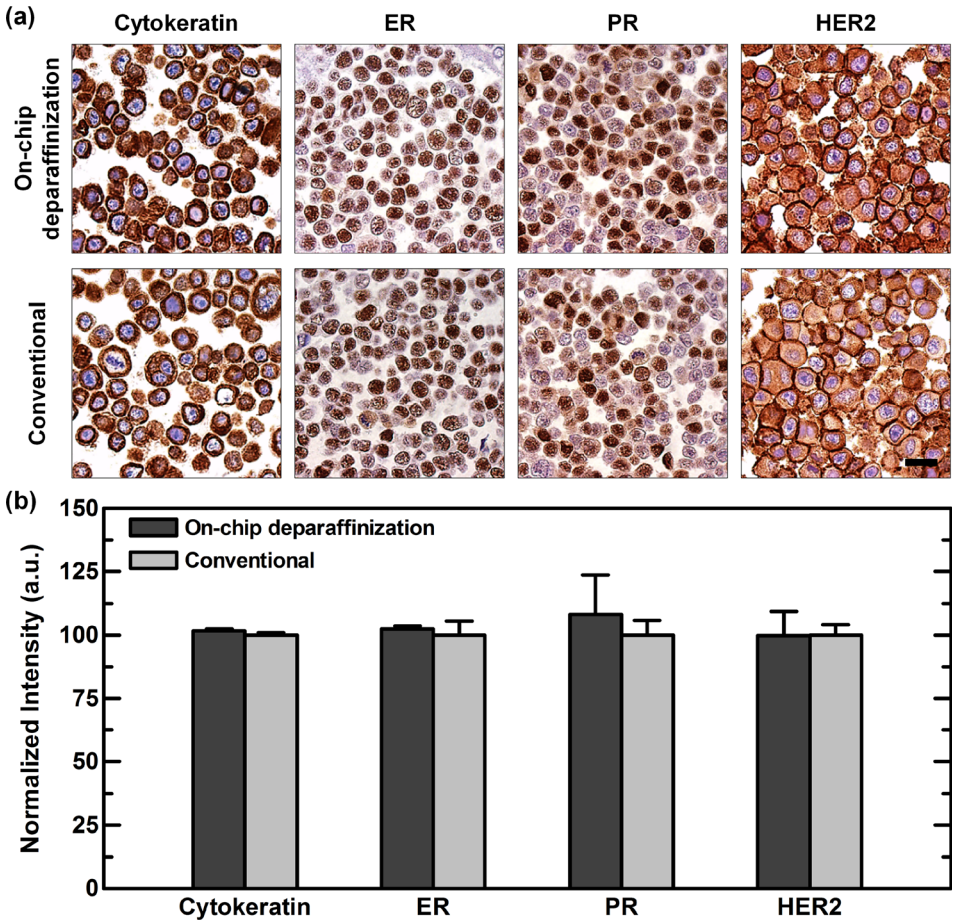

FIG. 3. Verification of the on-chip deparaffinization process by comparing the immunostaining result processed by on-chip and conventional deparaffinization. (a) Images of the immunostained breast cancer cell block sections for four biomarkers, including cytokeratin, ER, PR, and HER2 processed by on-chip and conventional deparaffinization (scale bar: 25 μm). (b) The quantitative analysis result of immunostained sections shows that the effect of on-chip deparaffinization is equivalent to the conventional method based on the immunostaining intensity. The error bars represent the standard deviation ($n = 6$).

dealing with the optimization of the heat-induced antigen retrieval, we have proceeded the verification to confirm the retrieval capability under low temperature conditions. The process time was fixed to 20 min, which was the identical condition with the conventional method to compare the retrieval capability. The effectiveness was verified based on immunostaining results. As expected, the immunostaining intensity increased as the temperature condition increased (Fig. S3 in the supplementary material), which corresponds to the previous research.[28,30] However, the injected retrieval solution into the PUA chip started to evaporate when the temperature condition was over 75 °C. Due to the enclosed environment of the on-chip process, in contrast to the conventional process, air bubbles generated during the heating process clogged the microchannel, resulting in a failure of the on-chip process. To prevent this situation, we set the temperature condition to 75 °C for conducting on-chip antigen retrieval.

The effectiveness of the on-chip antigen retrieval was also verified in a similar way, comparing the immunostaining results of three groups; one is processed by on-chip antigen retrieval, another processed by conventional antigen retrieval, and the other without antigen retrieval. All other IHC processes, including deparaffinization and immunostaining, were performed identically for three groups in a conventional manner. Figure 4(a) shows the immunostained sections

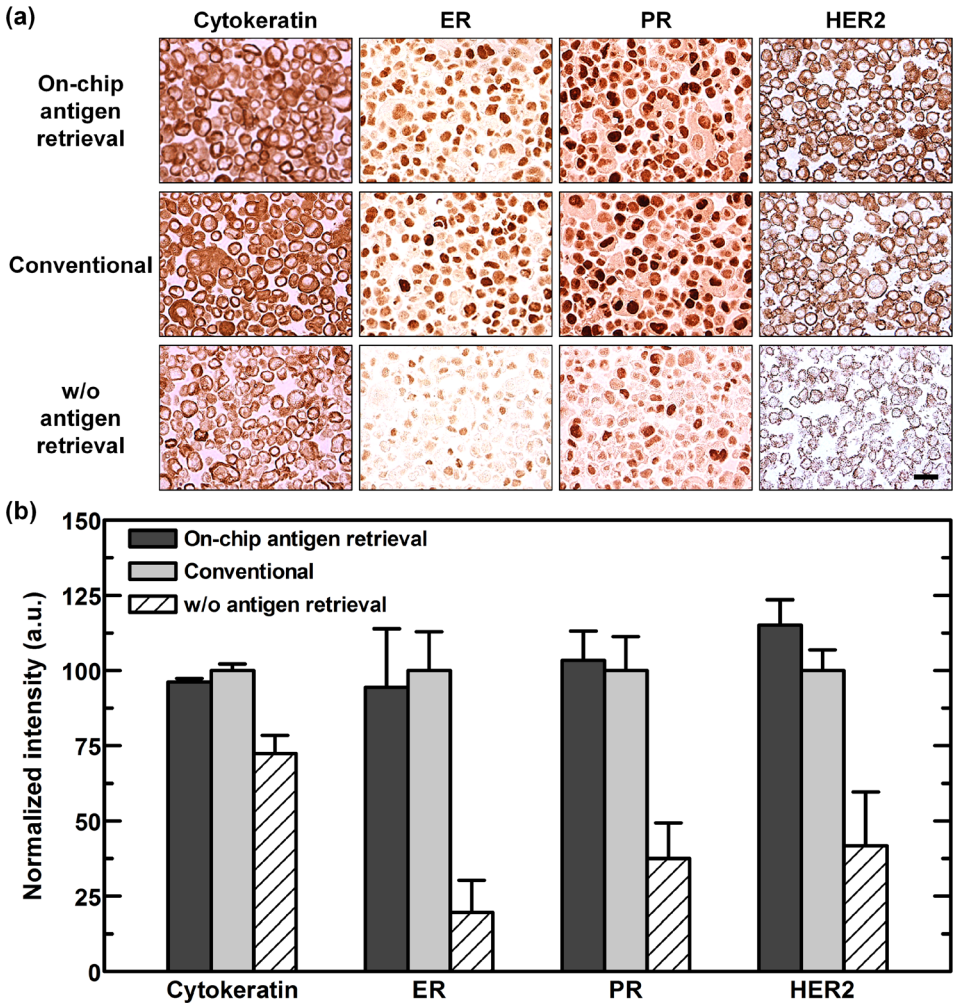

FIG. 4. Verification of the on-chip antigen retrieval process by comparing the immunostaining result processed by on-chip, conventional, and without antigen retrieval. (a) Images of the immunostained breast cancer cell block sections for four biomarkers, including cytokeratin, ER, PR, and HER2 processed by on-chip, conventional, and without antigen retrieval (scale bar: 25 μm). (b) The quantitative analysis result shows that the immunostaining intensity of the on-chip antigen retrieval group was similar to that of the conventional method group, whereas without the antigen retrieval group, the intensity was much lower. The error bars represent the standard deviation ($n = 5$).

processed by on-chip, conventional, and without antigen retrieval. As shown in Fig. 4(b), on-chip antigen retrieval showed comparable effectiveness against the conventional method based on the immunostaining results for four biomarkers on breast cancer cell sections. At the on-chip antigen retrieval condition, the normalized immunostaining intensities of cytokeratin, ER, PR, and HER2 were 96.09 ± 1.27, 94.34 ± 19.50, 103.35 ± 9.85, and 115.21 ± 8.28, respectively ($p > 0.5$ for ER and PR, $p > 0.05$ for cytokeratin, and $p < 0.05$ for HER2). Meanwhile, the immunostaining intensity without antigen retrieval was less than 75% compared to the conventional method. At the without antigen retrieval condition, the normalized immunostaining intensities of cytokeratin, ER, PR, and HER2 were 72.40 ± 6.11, 19.51 ± 10.77, 37.55 ± 11.90, and 41.68 ± 17.95, respectively ($p < 0.005$ for four biomarkers). Despite the lower temperature condition of the on-chip method than the conventional method (over 100 °C), this result indicates that the on-chip antigen retrieval has comparable retrieval capability with the conventional method. On the other hand, some variations of the effectiveness of on-chip antigen retrieval were observed for each biomarker. These variations can be caused by the difference in the optimal retrieval conditions between each biomarker, including temperature, pH, and time. Since our on-chip antigen retrieval was conducted at low temperature conditions, this can be compensated by increasing the process time and optimizing the retrieval reagents.

On-chip IHC processes performed on an FFPE section slide

After verification of two preparation processes of IHC, we performed on-chip IHC processes. Deparaffinization, heat-induced antigen retrieval, and immunoreaction processes were consecutively conducted on the same chip. Based on previous studies carried out at our laboratory, we set the process time for the incubation of the primary antibody for 20 min, while the conventional process takes 1 h. The process time for all other processes of on-chip IHC was also decreased in a similar ratio (1/3 to the conventional process time). For the negative control experiment, we performed an IHC assay using the anti-HER2 antibody against the MCF-7 breast cancer cell line that does not express HER2 and compared the results. Figure 5(a) shows the images of the immunostained sections processed by the on-chip and the conventional IHC processes. As shown in Fig. 5(b), the immunostaining result by on-chip IHC processes showed an equivalent result to the conventional IHC processes for the two biomarkers and negative control while reducing the total process time from 150 min to 60 min. On-chip IHC-based immunostaining intensities of cytokeratin, HER2, and negative control were 205.80 ± 4.55, 179.04 ± 12.49, and 16.51 ± 3.78, respectively, whereas conventional immunostaining intensities of cytokeratin, HER2, and negative control were 201.71 ± 4.48, 185.33 ± 3.75, and 17.87 ± 3.46, respectively ($p > 0.3$ for cytokeratin, HER2, and negative control). Despite the short process time, the staining signals for the two biomarkers were at least 10-fold higher than the negative control signal, indicating that the difference between positive expression and negative expression can be clearly distinguished. The accelerated process time, while maintaining the immunostaining quality, is mainly due to the enhanced reaction rate between the antigen and the antibody under the flow condition. The flow of the new antibody solution replaces the old antibody solution, which already reacts with the biomarker and has a lowered concentration, to maintain the reaction rate. The different immunostaining qualities of two biomarkers are considered to be due to the differences in antigen–antibody binding kinematics. The binding kinetics of each biomarker is quite different based on various factors, including the type, location, and binding affinity. By controlling the treatment time, flow rate, and reagent concentration, on-chip immunostaining results can be further improved, resulting in accurate cancer diagnosis.

HER2 classification of patient samples using on-chip IHC processes

The practical application of on-chip IHC processes to clinical cancer diagnosis was validated by testing our platform for human tissue samples. In this study, we focused on the HER2 classification, which classifies the HER2 expression level of patient tissue based on the IHC assay result. To validate this, on-chip IHC processes were performed on the patient tissue samples, and the immunostaining results were analyzed to confirm whether the HER2 expression level could be classified. Breast cancer patient tissues with different levels of HER2 expression

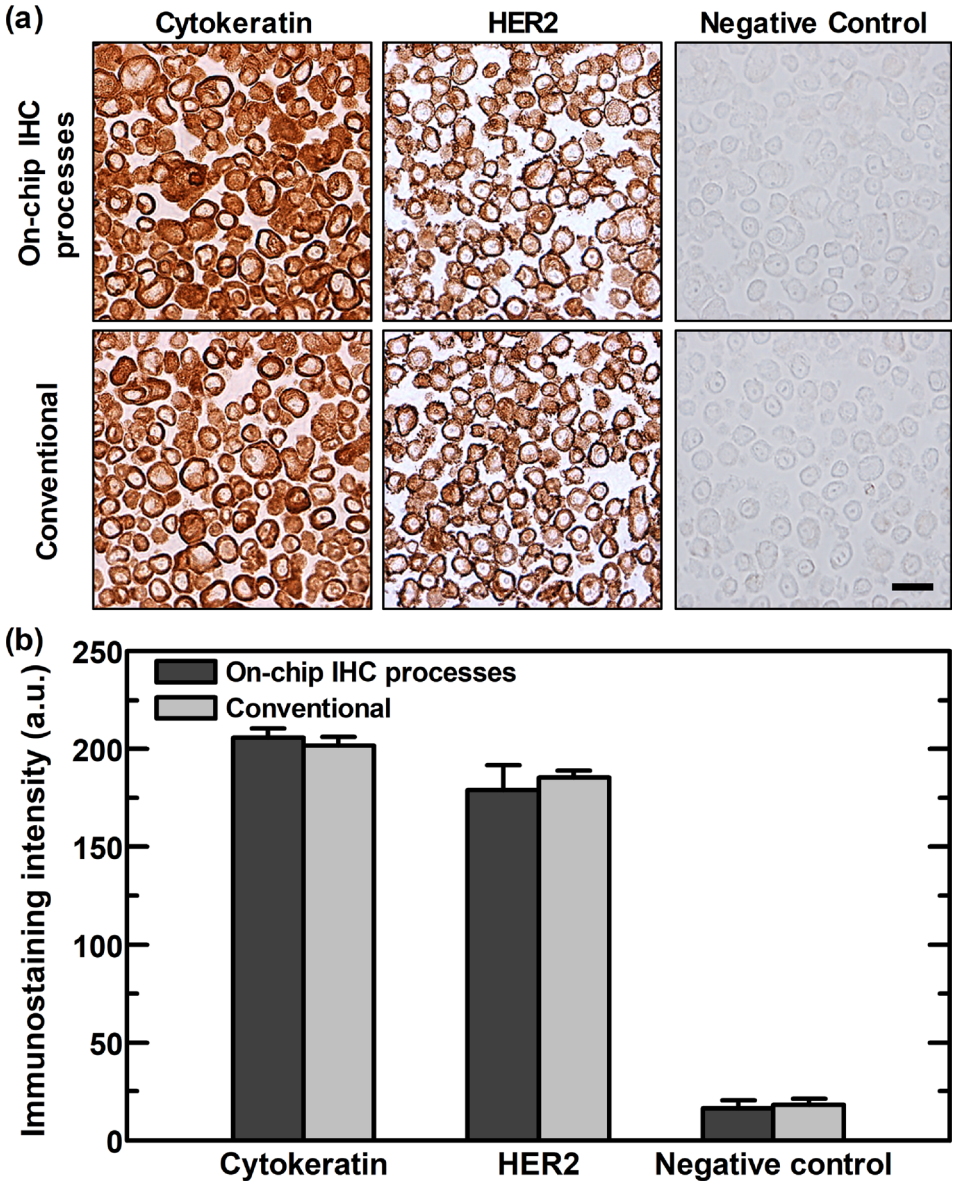

FIG. 5. Comparison of the on-chip IHC processes performed by the on-chip, conventional method and negative control. (a) Two biomarkers (cytokeratin and HER2) on breast cancer cell block-section slides immunostained by on-chip and conventional processes show a strong positive result, while the negative control shows no remarkable signal (scale bar: 25 μm). (b) The quantitative analysis result indicates that the on-chip IHC process shows an equivalent result compared to the conventional method and shows a clearly distinguishable result compared to the negative control. In addition, the whole process time was reduced to less than 1/2 (e.g., from 150 min to 60 min). The error bars represent the standard deviation ($n = 5$).

(negative, 1+, 2+, and 3+) were processed using our platform, and the immunostaining result was organized based on the ASCO/CAP guideline of HER2 expression by IHC assay.[31] Figures 6(a)–6(c) show the images of the immunostained tissue section with HER2 1+, 2+, and 3+ expression levels, respectively. The images of immunostaining on patient tissue sections show significant differences according to the HER2 expression level (immunostaining intensities of HER2 1+, 2+, and 3+ were 6.67 ± 3.47, 27.36 ± 1.48, and 97.18 ± 22.23, respectively, $^*p < 0.005$), which can be confirmed by quantitative analysis in Fig. 6(d). This result implies that our platform can be used to make precise diagnosis of HER2-positive breast cancer, and it shows that an accurate IHC assay can be performed not only on cell block sections but also on patient tissue sections. If it is provided with an optimized protocol for each disease and

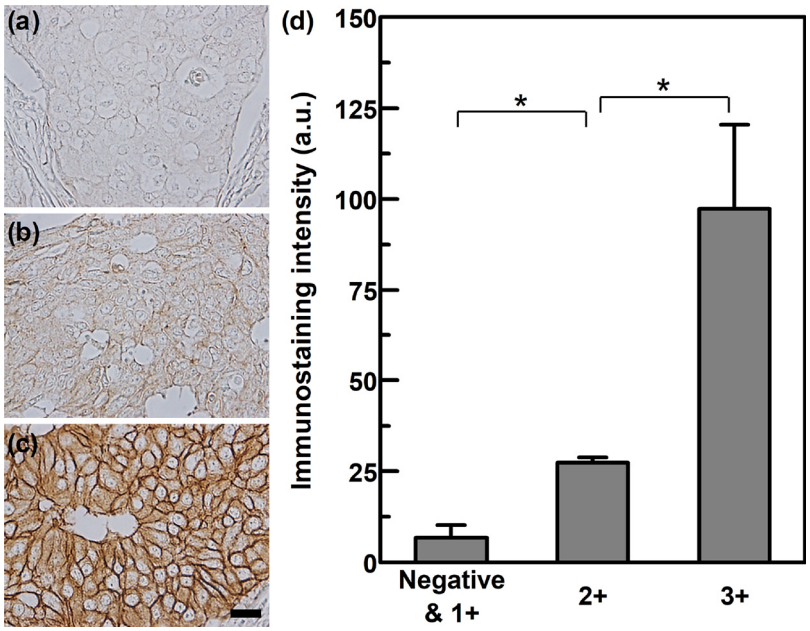

FIG. 6. HER2 classification of breast cancer tissue samples using on-chip IHC processes. The images of the breast cancer tissue section with (a) HER2 1+, (b) 2+, and (c) 3+ expression levels immunostained by on-chip IHC processes show a distinct difference in immunostaining results according to the HER2 expression level ($*p < 0.005$). (d) The quantitative analysis result shows that the HER2 classification can be successfully performed using on-chip IHC processes. The error bars represent the standard deviation ($n = 5$).

biomarker, it can be applied in the actual medical field. Combined with multiple biomarker detection techniques by channel multiplexing and/or multi-fluorescence labeling, a high throughput microfluidic-based cancer diagnosis platform can be proposed.

CONCLUSIONS

We first demonstrated a microfluidic platform to perform the on-chip IHC processes consecutively. A narrow channel wall structure of the chip, which is important to provide a conformal contact, facilitated the pressure-based reversible assembly of a rigid PUA chip with a section slide and showed no leakage or damage to the slide. The organic solvent used in the deparaffinization process, which was one of the limitations of PDMS-based microfluidic integration to IHC, was handled on our PUA-based microfluidic chip without any deformation or failure. On-chip deparaffinization showed a reduced process time due to the convection of the solvent to enhance the dissolution of paraffin from the FFPE section slide. A temperature-controllable platform enabled on-chip heat-induced antigen retrieval and showed a comparable effect on the conventional method even at low temperature conditions. The on-chip IHC process on the breast cancer cell section slide showed an equivalent immunostaining result and reduced process time compared to the conventional method. Further optimization of each IHC process will contribute to the enhancement of the immunostaining result, which is essential for an accurate diagnosis of cancer. In the experiment using breast cancer tissue sections, the HER2 expression level was clearly classified according to the immunostaining intensity, indicating the possibility of immediate application to the medical field. Unlike the existing microfluidic IHC platform, the PUA chip-based on-chip IHC can directly handle paraffin-embedded sections without any preparation steps, allowing end users to easily use them. Our on-chip IHC platform enables to provide versatile immunostaining conditions by controlling process time, flow velocity, concentration of reagents, and temperature, as if the researchers were optimizing the process conditions. Using the chemical properties of the PUA chip, it can be used for assay and analysis in harsh environments using various solvents and the IHC assay conducted in this

study. Due to the durability of PUA, the PUA chip can be used semi-permanently if there is no structural damage by the physical impact. In addition, since the PUA chip used in this study is the most basic chamber-type microfluidic chip, it is simple to expand the potential by incorporating the structure and function of the microfluidic chip proposed in other studies. We expect this microfluidic platform to offer practical applications of microfluidics for the various miniaturized, automated diagnostic platforms.

SUPPLEMENTARY MATERIAL

See supplementary material for a detailed description of the fabrication process of the PUA chip (Fig. S1), comparison of the pressure-based reversible sealing in a microfluidic PUA chip (Fig. S2), and verification of the temperature condition of the on-chip heat-induced antigen retrieval based on the immunostaining result (Fig. S3).

ACKNOWLEDGMENTS

This research was supported by the National Research Foundation of Korea (NRF) (Nos. NRF-2016R1A2B3015986, NRF-2015M3A9B3028685, and NRF-2017M3A7B4039936) funded by the Ministry of Science and ICT.

[1]E. de Boer, J. M. Warram, M. D. Tucker, Y. E. Hartman, L. S. Moore, J. S. de Jong, T. K. Chung, M. L. Korb, K. R. Zinn, G. M. van Dam, E. L. Rosenthal, and M. S. Brandwein-Gensler, Sci. Rep. **5**, 10169 (2015).
[2]R. D. Odze, M. A. Marcial, and D. Antonioli, Hum. Pathol. **27**, 896–903 (1996).
[3]F. M. Blows, K. E. Driver, M. K. Schmidt, A. Broeks, F. E. van Leeuwen, J. Wesseling, M. C. Cheang, K. Gelmon, T. O. Nielsen, C. Blomqvist, P. Heikkilä, T. Heikkinen, H. Nevanlinna, L. A. Akslen, L. R. Bégin, W. D. Foulkes, F. J. Couch, X. Wang, V. Cafourek, J. E. Olson, L. Baglietto, G. G. Giles, G. Severi, C. A. McLean, M. C. Southey, E. Rakha, A. R. Green, I. O. Ellis, M. E. Sherman, J. Lissowska, W. F. Anderson, A. Cox, S. S. Cross, M. W. R. Reed, E. Provenzano, S.-J. Dawson, A. M. Dunning, M. Humphreys, D. F. Easton, M. García-Closas, C. Caldas, P. D. Pharoah, and D. Huntsman, PLoS Med. **7**, e1000279 (2010).
[4]M. Wachtel, T. Runge, I. Leuschner, S. Stegmaier, E. Koscielniak, J. Treuner, B. Odermatt, S. Behnke, F. K. Niggli, and B. W. Schäfer, J. Clin. Oncol. **24**, 816–822 (2006).
[5]J. M. Harvey, G. M. Clark, C. K. Osborne, and D. C. Allred, J. Clin. Oncol. **17**, 1474–1481 (1999).
[6]M. Cregger, A. J. Berger, and D. L. Rimm, Arch. Pathol. Lab. Med. **130**, 1026–1030 (2006), see http://www.archivesofpathology.org/doi/full/10.1043/1543-2165%282006%29130%5B1026%3AIAQAOP%5D2.0.CO%3B2.
[7]V. Guinard-Samuel, A. Bonnard, P. De Lagausie, P. Philippe-Chomette, C. Alberti, A. El Ghoneimi, M. Peuchmaur, and D. Berrebi-Binczak, Mod. Pathol. **22**, 1379–1384 (2009).
[8]C. M. J. Conklin, K. J. Craddock, C. Have, J. Laskin, C. Couture, and D. N. Ionescu, J. Thorac. Oncol. **8**, 45–51 (2013).
[9]D. Gonzalez de Castro, P. A. Clarke, B. Al-Lazikani, and P. Workman, Clin. Pharmacol. Ther. **93**, 252–259 (2013).
[10]D. K. Nomura, M. M. Dix, and B. F. Cravatt, Nat. Rev. Cancer **10**, 630–638 (2010).
[11]L. A. Niemeier, D. J. Dabbs, S. Beriwal, J. M. Striebel, and R. Bhargava, Mod. Pathol. **23**, 205–212 (2010).
[12]B. J. Chae, J. S. Bae, A. Lee, W. C. Park, Y. J. Seo, B. J. Song, J. S. Kim, and S. S. Jung, Jpn. J. Clin. Oncol. **39**, 217–224 (2009).
[13]A. H. C. Ng, U. Uddayasankar, and A. R. Wheeler, Anal. Bioanal. Chem. **397**, 991–1007 (2010).
[14]K. F. Lei, J.-L. Liu, C.-H. Huang, R.-L. Kuo, and N.-M. Tsang, BioChip J. **10**, 34–41 (2016).
[15]M. S. Kim, T. Kim, S.-Y. Kong, S. Kwon, C. Y. Bae, J. Choi, C. H. Kim, E. S. Lee, and J.-K. Park, PLoS One **5**, e10441 (2010).
[16]M. S. Kim, S. Kwon, T. Kim, E. S. Lee, and J.-K. Park, Biomaterials **32**, 1396–1403 (2011).
[17]R. D. Lovchik, G. V. Kaigala, M. Georgiadis, and E. Delamarche, Lab Chip **12**, 1040–1043 (2012).
[18]A. H. Ng, M. D. Chamberlain, H. Situ, V. Lee, and A. R. Wheeler, Nat. Commun. **6**, 7513 (2015).
[19]S. Kim, S. Kwon, C. H. Cho, and J.-K. Park, Lab Chip **17**, 702–709 (2017).
[20]S. Kwon, M. S. Kim, E. S. Lee, J. S. Sohn, and J.-K. Park, Integr. Biol. **6**, 430–437 (2014).
[21]S. Kwon, C. H. Cho, E. S. Lee, and J.-K. Park, Anal. Chem. **87**, 4177–4183 (2015).
[22]A. T. Ciftlik, H.-A. Lehr, and M. A. M. Gijs, Proc. Natl. Acad. Sci. U. S. A. **110**, 5363–5368 (2013).
[23]S. Brajkovic, D. G. Dupouy, L. de Leval, and M. A. Gijs, Lab. Invest. **97**, 983–991 (2017).
[24]S. Kwon, C. H. Cho, Y. Kwon, E. S. Lee, and J.-K. Park, Sci. Rep. **7**, 45968 (2017).
[25]J. N. Lee, C. Park, and G. M. Whitesides, Anal. Chem. **75**, 6544–6554 (2003).
[26]J. F. Cors, A. Kashyap, A. F. Khartchenko, P. Schraml, and G. V. Kaigala, PLoS ONE **12**, e0176691 (2017).
[27]S. J. Choi, P. J. Yoo, S. J. Baek, T. W. Kim, and H. H. Lee, J. Am. Chem. Soc. **126**, 7744–7745 (2004).
[28]S. R. Shi, M. E. Key, and K. L. Kalra, J. Histochem. Cytochem. **39**, 741–748 (1991).
[29]S. A. Pileri, G. Roncador, C. Ceccarelli, M. Piccioli, A. Briskomatis, E. Sabattini, S. Ascani, D. Santini, P. P. Piccaluga, O. Leone, S. Damiani, C. Ercolessi, F. Sandri, F. Pieri, L. Leoncini, and B. Falini, J. Pathol. **183**, 116–123 (1997).
[30]P. Evers and H. B. M. Uylings, J. Histochem. Cytochem. **42**, 1555–1563 (1994).
[31]A. C. Wolff, M. E. H. Hammond, D. G. Hicks, M. Dowsett, L. M. McShane, K. H. Allison, D. C. Allred, J. M. S. Bartlett, M. Bilous, P. Fitzgibbons, W. Hanna, R. B. Jenkins, P. B. Mangu, S. Paik, E. A. Perez, M. F. Press, P. A. Spears, G. H. Vance, G. Viale, and D. F. Hayes, J. Clin. Oncol. **31**, 3997–4013 (2013).